International Journal of Scientific & Engineering Research, Volume 4, Issue 5, May-2013
ISSN 2229-5518

Impart Of Wall Geometry On Thermal Distribution Behind A Diffracted Shock Wave

Muritala A.O.*, Popoola,O.T. and Adio, S.A
Department of Mechanical Engineering, Obafemi Awolowo University, Ile-Ife, Nigeria
* muriadam@oauife.edu.ng

Abstract— The effect of wall geometry on thermal distribution behind a diffracted shock wave is investigated using experimentally validated numerical code. Initial experiments examined the flow interaction at a range of incident shock Mach numbers 1.5 on 90^o corner wall. The results of the flow interactions were used to validate the numerical code that is used in the present analysis. The temperature of the flow behind the original incident shock wave was very high until the start of the diffraction process. The diffraction of the incident shock wave at the curved/corner region motivated the formation of weak shock waves and a shear layer which combined to produce a complex flow structure. The flow temperature dropped significantly within the complex flow domain attaining its minimum at the corner/curvature due to sudden expansion of the flow. For curved walls, temperature decreases from the start of the wall curvature sweeps downstream with the movement of the complex flow region. The reflection of the incident shock interacted with the flow and triggered sudden increase of temperature at a region along the wall. This local rise and fall in temperature creates thermal stress on the wall. This occurrence requires special attention in the design of thermal devices for high speed flows.

Index Terms— Compressible flow, shock wave diffraction, shear layer, flow separation

1 INTRODUCTION

The investigation of temperature distribution behind a diffracted shock wave is motivated by the rapid increase in speed of modern supersonic flow devices. The design of such devices usually requires thermal property of the material due to thermal stress imposed on the wall surface by the flow. The inherent characteristic of high speed flows is the formation of shock waves which are mechanical waves of finite amplitude propagated over a very short period of time.

A planar shock wave that moves over a convex geometry will be affected by series of disturbance waves that will affect the shape, the strength and the orientation of the shock. This process is described as shock wave diffraction [1]. The flow behind the diffracted shock may become locally supersonic depending on the initial conditions of the incident shock wave [2].

A shear layer which is a line of finite discontinuity of temperature and velocity evolved as the flow separates from the wall due to the presence of adverse pressure gradient along the surface of the wall. The resulting flow becomes complex as a result of the combination of shear layer, and weak shock waves as earlier observed by Skews [3, 4] and confirmed by Muritala [5].

Earlier works [3, 4] examined shock wave diffraction over corner walls for different flow conditions. Separation was observed even at very low angle and many flow features such as oblique shock, shear layer, recompression shock and vortex were observed. The temperature distribution was not explained for any of the tests conducted in the shock tube.

Large scale experiments have been conducted to explain the flow features behind the diffracted shock wave [6]. It was noticed that there is a significant difference between large scale experimental data and the data obtained from the conventional shock tubes. The images of flow interaction in the large scale tests were comparable to the numerical results obtained when using SST k-ω turbulent model. The temperature history was not recorded for both experimental and numerical analysis, however, the pressure history was comparable for the Mach numbers considered.

A very challenging task in shock tube experiments is the determination of temperature history within the flow domain. The propagation of the shock gives rise to high temperature, but there is rapid and non uniform temperature distribution behind the diffracting shock wave. The use of thermocouples for temperature measurement of a transient (order of 1μs) non-uniform flow behind a diffracting shock wave is a problem still under investigation. Other option used by earlier researchers involves viewing a continuous light source through a hot gas containing a metal vapor. The quantitative value of temperature at certain point is obtained using spectrum line reversal technique. The heat energy transferred to the wall of the shock tube or solid object immersed in the flow can be measured by thin thermocouples and thin film of metal attached to an insulating back [7]. However, the size of the thermocouple to be used for high Mach number incident shock is still a challenge.

The present investigation examined the diffraction process using a numerical code that was validated by the results of some tests conducted in a shock tube. The incident shock Mach numbers considered ranged between 1.4 and 3.0, and the diffraction process was considered on both curved and corner walls. The contour of temperature distributions within the complex flow structure behind the diffracted shock wave is used for the analysis.

2 METHODOLOGY

2.1 Numerical Computation

The flow domain is defined by length L which is the length of the corner through which the shock diffracts. The inlet boundary is 4L in height and about 4L from the corner. This is to ensure the damping out of numerical noise due to impulsive start of the flow. The outlet boundary is 8L from the corner to avoid undesirable interaction. The flow domain is discretized using unstructured quadrilateral and triangular cells with initial dimension of 0.002mm.

The y^+ value of the cell nearest to the wall around the corner is set to 11.63 in the region under the shear layer so that the boundary layer could be properly resolved. This lies within the recommended value range of $5 \leq y^+ \leq 30$ specified for the models used [8].This is particularly important as the global flow features that are of interest are strongly influenced by this. The values of y^+ at other boundaries is greater than 11.63, but less than 100 in order not to increase the computational resources required for the simulations.

The flow is governed by the mathematical equations based on the fundamental fluid dynamic principles; mass conservation, conservation of momentum and conservation of energy. The density and pressure are related by the perfect gas law; this is justified by the fact that the maximum temperature is well below 1000K for the incident shock Mach numbers tested. The flow governing equations are the Navier – Stokes equations, and the energy equation coupled through the density–pressure relationship.

For the present application the ideal gas equation is written as follows:

$$\rho = \frac{p_{op} + p}{\frac{R}{m}T} \qquad (1)$$

where p_{op} is the operating pressure, p is the static pressure, R is the universal gas constant, M is the molecular weight and T is the temperature.

For ideal gas, the total pressure and temperature are related to static pressure and temperature by:

$$\frac{To}{T} = (1 + \frac{\gamma+1}{2}M^2) \qquad (2)$$

$$\frac{Po}{P} = (1 + \frac{\gamma+1}{2}M^2)^{\frac{\gamma}{\gamma-1}} \qquad (3)$$

It is important to mention here how energy is taken care of in the analysis. Heat transfer takes place between the gas molecules and between the gas and the wall of the shock tube. The energy equation is written as:

$$\frac{\partial}{\partial t}(\rho E) + \nabla.\left(v(\rho E + p)\right) = \nabla.\left(K\nabla T - \sum_j H_j D_j + (\bar{\bar{\tau}}.\vec{v})\right) \qquad (4)$$

The first three terms on the right hand side represents energy transfer due to conduction, species diffusion and viscous dissipation:

where $E = h - \frac{p}{\rho} + \frac{v^2}{2}$

and h is the sensible enthalpy.

The flow domain around the geometry of interest can be divided into three regions based on Prandtl hypothesis: the laminar sub-layer where the fluid closest to the wall is dominated by viscous shear ($y^+ < 5$), the boundary layer where the effect of viscosity varies with distance from the adjacent surface ($5 < y^+ < 100$) and inertial dominated region in which viscous effects is not significant [8]. The present study is largely inviscid flow except near the wall where viscous effects play a significant role.

2.2 Solution Procedure

In setting up the simulation, the 2 – dimensional coupled density based solver of Fluent 6.3 was used with energy equation. The gradient option was cell based and the k - turbulent model was enabled in the solver. The material chosen was air and the ideal gas law was selected to compute density. The operating condition was set at zero pressure for the reference position defined by x = 0 and y = 0, the gravity along y –axis was set at 9.81m/s2 and the operating density used was 1.225kg/m3 . The boundary conditions were given as total gauge pressure, and initial gauge pressure which is the static pressure used in Fluent for solution initialisation to provide initial guess of the velocity. The input for the total temperature is the stagnation temperature and the turbulent flow parameters were given according to the Fluent 6.3 prescriptions. The outlet flow conditions were the ambient conditions fixed at 0.833Kpa and 293K for pressure and temperature respectively. The solution was initialised from inlet relative to the cell zone and the system was patched by the ambient flow conditions earlier stated. The gradient adaption was performed by fixing values for coarsen and refine threshold using different adaption stages. This is a very important step in the formulation because it determines the independent of the solution from the meshing. 42

The system described above initiated a normal shock wave of a known Mach number which was propagated through a stationary air. It travelled a considerable distance before encountering the convex corner from which the diffraction process commenced. Series of simulations using different pressure settings were carried out following the steps explained above. Solutions were obtained at different incident shock Mach numbers and for different solvers. The results were obtained in form of velocity, pressure and density contours as well as the velocity vector using the post processing facilities in Fluent.

3 RESULTS AND DISCUSSION

The diffraction of an incident shock Mach number 1.5 on the 90°convex wall is shown in Figure 1. This particular case is the benchmark proposed by Takayama and Inoue [9] to measure the performance of CFD codes. Figure 1(a, b and c) are experimental images at different diffraction times [5] and Figure 1(d, e and f) are results from the SST k - ω turbulent

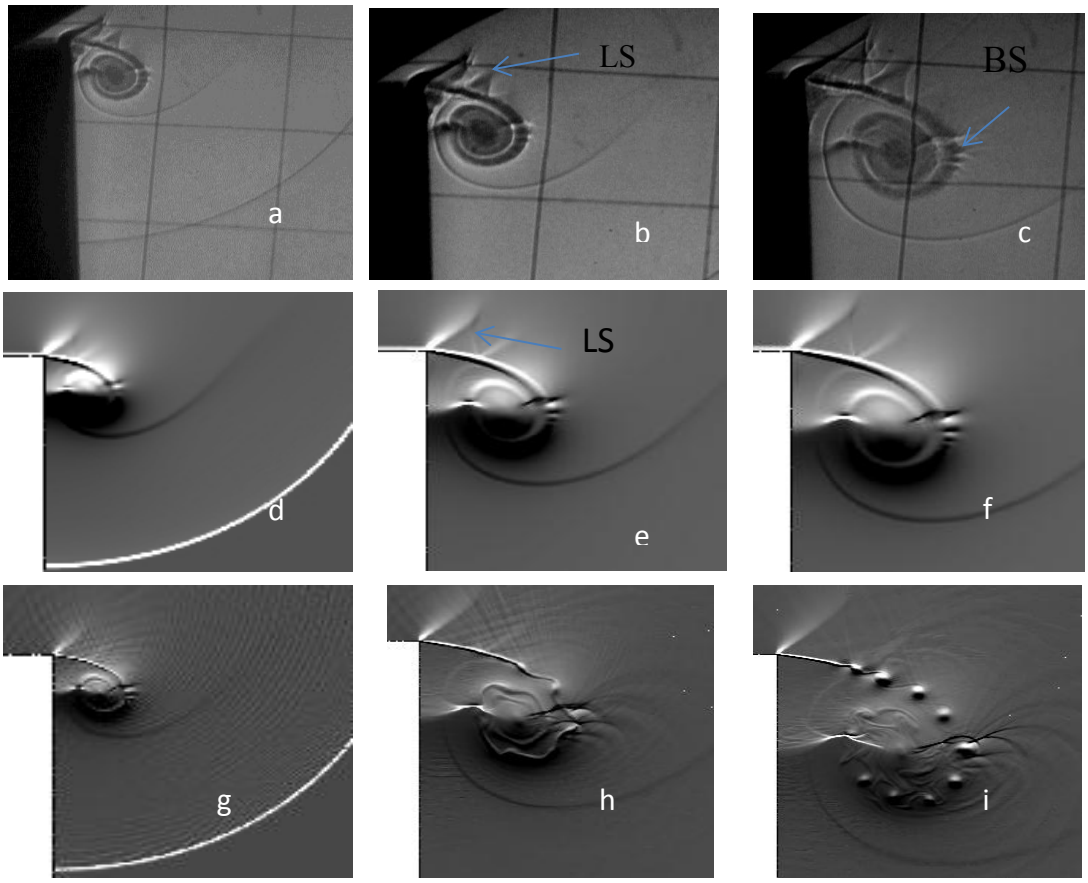

Figure 1: Comparison of experimental result of (Muritala, 2011) (a-c), SST K-ω turbulent model (d-f) and Laminar Navier-Stokes solver for incident shock Mach number 1.5.

model while Figure 1(g, h and i) are from Navier–Stokes solver with laminar boundary conditions.

The flow features of interest are: shear layer, lambda shocks (LS), the vortex, the bifurcated shocks (BS) on the vortex, and the contact surface. The comparison of the images in Figure 2 is based on the length of the flow feature of interest measured at time t which is expressed in a non-dimensional form as shown in equation (5). For experimental pictures the length of the relevant flow feature is determined using the square grids superimposed on the test window of the shock tube used by Muritala [5]. Each of the grids is 50mm in dimension, and the approximate dimension of the flow features are obtained from the grid spacing.

The dimensionless time scale is given by τ:

$$\tau = \frac{at}{c} \qquad (5)$$

where L is the characteristic length, t is the time from the start of diffraction process to the formation of the flow feature of interest, a is the sound speed in the undisturbed region ahead of the incident shock wave.

There is a good agreement in the bench mark results between the current experimental images and results of the SST k - ω turbulent model. The lambda shocks are well predicted with the bifurcated shock that is interacting with the vortex. The contact surface and vortex are also comparable with the experiment. The pattern by which the shear layer rolled up into a spiral vortex is the same for all the images.

The laminar Navier–Stokes images show instability along the shear layer at later times. This instability as it develops rolled up into a spiral vortex, followed by the breaking up of the shear layer into vortices as shown in figure 1h&i. These developments follow a similar pattern with the Euler solutions as earlier observed [10] [11], except that it occurred at later times in laminar Navier–Stokes results.

Figure 2 compared transient development of the vortex for different numerical codes. It is observed that the vortex size increases with time but the result of SST k-ω turbulent model predicted the vortex better than the other numerical model.

Figure 3a shows the movement of the shock within the flow domain of interest. At the instant of shock propagation the temperature increases and is uniformly distributed as shown in Figure 3a. The shock moves further and encounter a convex bend where it diffracted and developed complex flow structure due to combination of weak shock waves and shear layer. The numerical schlieren result of the complex flow structure behind a diffracted shock wave is shown in Figure 4.

The diffraction of the shock at the convex bend induces the flow structure that is accompanied by non uniform temperature distribution. The temperature along the curvature dropped to ambient temperature as shown in

Figure 3b, and changes as the diffraction progresses further downstream. The original incident shock is reflected from the wall downstream of the curvature and this reflected shock interacts with the flow along the curved region (Figure 3c). This interaction motivates sudden rise in temperature at a particular location along the curved wall

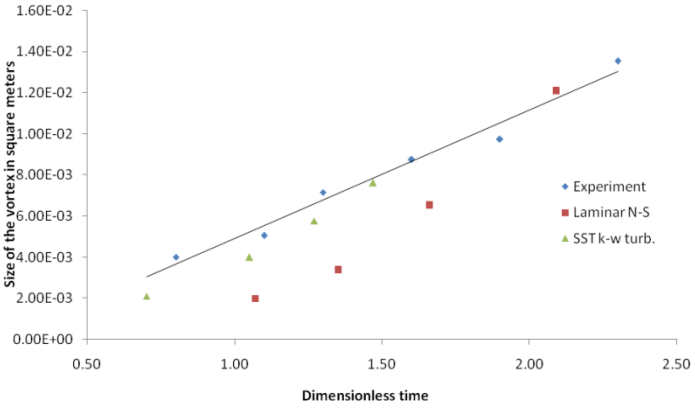

Figure 2 Experimental, Laminar Navier-Stokes solver and SST-k-ω turbulence model showing transient development of the vortex.

Further movement of the shock towards the outlet leads to formation of high temperature region along the curvature. This hot spot can attain any temperature depending on the initial incident shock strength. Since this hot region is not fixed along the wall then thermal stress along the curvature changes with time. It is important to note that after the start of diffraction the original high temperature along the wall has reduced substantially as shown in Figure 3d. This shows that introduction of an obstacle along the wall geometry can greatly modify the thermal stress on the wall of high speed flow devices.

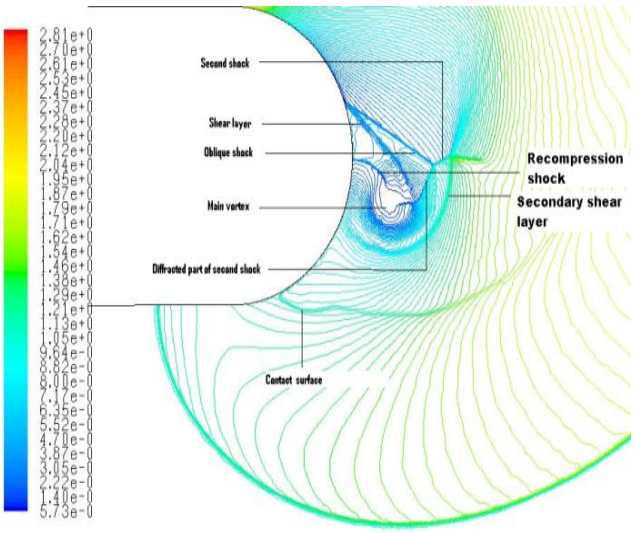

Figure 4: Complex flow features on curved wall at incident shock Mach number greater than 1.5

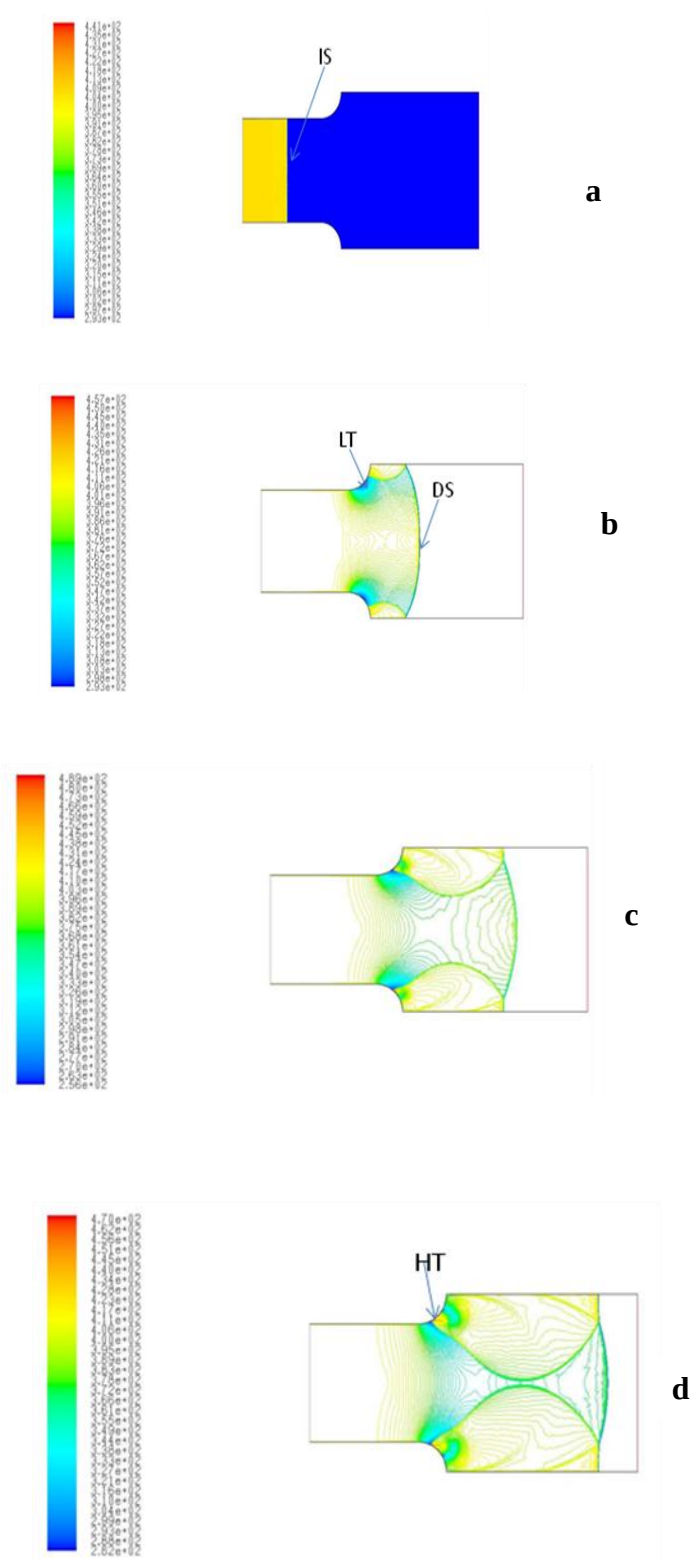

Figure 3: The contour of temperature behind a diffracted shockwave of initial Mach number 1.6
IS-Incident shock wave, **LT**-Low temperature region, **HT**-High temperature region, **DS**-Diffracted shock wave

4 Conclusion

The thermal distribution behind a diffracted shock wave has been investigated. The analysis shows that the thermal distribution behind a diffracted shock wave is unsteady. The temperature distribution changes significantly behind a diffracted shock wave from original high temperature that is uniformly distributed to a non uniform profile. The diffracting surface experiences hot region that moves along the wall. The wall thermal stress changes with time.

References

[1] G. Ben-Dor, O. Igra and T. Elperin, Handbook of shock waves, vol. 1, San Diego: Academic Press, 2012.

[2] B. Skews, "Shock wave diffraction on mult - faceted and curved walls," *Shock waves,* vol. 3, no. 14, pp. 137 - 146, 2005.

[3] B. Skews, "The shape of diffracting shock wave," *Journal of Fluid Mechanics,* vol. 29, pp. 297 - 304, 1967a.

[4] B. Skews, "The perturbed region behind a diffracting shock wave," *Journal of Fluid Mechanics,* vol. 29, p. 705, 1967b.

[5] A. Muritala, "Separation of Compressible flows over convex walls, PhD Thesis,," University of the Witwatersrand,, South Africa, 2011.

[6] A. Muritala, C. Law and B. Skews, "Shock wave diffraction on convex curved walls," in *In proceeding 28th International Symposium on Shock waves*, Manchester, 2011.

[7] W. C. Marlow, "Utilization of Thermocouples as Heat Transfer Gauges," Sunnyvale, California, 1959.

[8] H. Versteeg and W. Malalasekera., An introduction to computational fluid dynamics: the finite volume method, England: Addison Wesley Longman Limited, 1995.

[9] K. Takayama and O. Inoue, "Large scale shock wave diffraction experiments," in *29th International Congress on High-Speed Photography and Photonics*, Moricha, Japan,, 2010.

[10] K. Takayama and O. Inoue, "Shock wave diffraction over a 90 degree sharp corner," in *Posters Presented at 18th International Symposium on Shock Waves ISSW*, 1991.